© 2016. Published by The Company of Biologists Ltd | Journal of Cell Science (2016) 129, 354-366 doi:10.1242/jcs.174284

RESEARCH ARTICLE

FGF control of E-cadherin targeting in the *Drosophila* midgut impacts on primordial germ cell motility

Guillem Parés and Sara Ricardo*

ABSTRACT

Embryo formation requires tight regulation and coordination of adhesion in multiple cell types. By undertaking imaging, three-dimensional (3D) reconstructions and genetic analysis during posterior midgut morphogenesis in *Drosophila*, we find a new requirement for the conserved fibroblast growth factor (FGF) signaling pathway in the maintenance of epithelial cell adhesion through FGF modulation of zygotic E-cadherin. During *Drosophila* gastrulation, primordial germ cells (PGCs) are transported with the posterior midgut while it undergoes dynamic cell shape changes. In embryos mutant for the FGF signaling pathway components Branchless and Breathless, zygotic E-cadherin is not targeted to adherens junctions, causing midgut pocket collapse, which impacts on PGC movement. We find that the ventral midline also requires FGF signaling to maintain cell–cell adhesion. We show that FGF signaling regulates the distribution of zygotic E-cadherin during early embryonic development to maintain cell–cell adhesion in the posterior midgut and the ventral midline, a role that is likely crucial in other tissues undergoing active cell shape changes with higher adhesive needs.

KEY WORDS: *Drosophila*, E-cadherin, FGF, PGC, Cell adhesion, Midgut

INTRODUCTION

Morphogenesis and the formation of specialized structures is the basis of embryonic development. Epithelial integrity during morphogenesis cannot take place without correct regulation of cell adhesion. Maintenance of strong cell adhesion is especially important in tissues that undergo dynamic tissue movements for the formation of complex three-dimensional (3D) structures. E-cadherin, encoded by the *shotgun* (*shg*) gene in *Drosophila*, is a core adherens junctions component and a key mediator of cell adhesion. *Drosophila* E-cadherin (DE-cadherin; from here onwards called E-cadherin for simplicity) is maternally provided and ubiquitously expressed during early stages of embryogenesis. In *Drosophila*, tissues that undergo substantial dynamic cell rearrangements and movements, such as the ventral ectoderm, require both maternal and zygotic E-cadherin (Tepass et al., 1996; Uemura et al., 1996). However, the contribution and regulation of newly synthesized zygotic E-cadherin in early morphogenetic movements, which take place shortly after the embryonic maternal to zygotic transition, is currently unknown. Moreover, trafficking of newly produced E-cadherin has only been directly shown in MDCK and HeLa cells *in vitro*, where it travels through Rab11-positive vesicles (Desclozeaux et al., 2008; Lock and Stow, 2005). How newly produced E-cadherin traffic is regulated across systems and *in vivo* is presently unknown. In *Drosophila*, the posterior midgut epithelium (pmg) invaginates forming a round cavity at its blind end, the posterior midgut lumen. At the exact same time, the primordial germ cells (PGCs), formed outside the embryo, are taken inside the embryo forming a cluster inside the pmg cavity. These events are highly linked and proper adhesion of PGCs to midgut cells (DeGennaro et al., 2011) and remodeling of midgut cells (Seifert and Lehmann, 2012) are required, respectively, for correct PGC internalization inside the embryo and PGC motility, which, in turn, is necessary for functional gonad formation. Therefore, strong cell adhesion of the pmg epithelia needs to be maintained during the dynamic movements of midgut morphogenesis while simultaneously creating and maintaining a pocket to transport the clustered PGC inside of the embryo. We found that the fibroblast growth factor (FGF) ligand Branchless (Bnl) regulates cell adhesion in the pmg epithelium necessary for tissue organization and correct PGC clustering and movement across the epithelium.

The *Drosophila* genome encodes only two FGF receptors, Hearthless (Htl) and Breathless (Btl). Htl is required for mesoderm migration and is activated by one of its ligands Thisbe (Ths) and Pyramus (Pyr), and Btl, expressed in ectodermal and endodermal tissues, is exclusively activated by Bnl.

FGF signaling is a widely used, conserved signaling pathway required in cell proliferation, survival, differentiation and migration (Muha and Muller, 2013). In vertebrate systems, FGF-dependent induction of cell migration is often linked to its role in epithelial-to-mesenchymal transition (EMT) with loss of cell adhesion and cell polarity that defines EMT (Thiery et al., 2009). However, it has been recently appreciated that FGF might also function to maintain cell adhesion. In vertebrates, FGF signaling is needed in the maintenance of interendothelial adhesion (Murakami et al., 2008) and, in *Drosophila*, it has been suggested that Htl signaling maintains cell adhesion during mesoderm migration, in addition to its role in migration (Bae et al., 2012).

In this study, we show that the FGF receptor Btl is expressed in the pmg and together with its ligand, Bnl, is required for pmg 3D tissue architecture through a new and unexpected role in modulation of zygotic E-cadherin and maintenance of epithelial cell adhesion.

RESULTS

Bnl and Btl signaling impacts on PGC motility

In a search for PGC motility regulators, we found that embryos mutant for the FGF ligand and receptor pair *bnl* and *btl* showed defective PGC movement. We analyzed embryos mutant for a *btl* hypomorph allele ($btl^{H82\Delta3}$), as the null allele (btl^{LG9}) showed embryonic patterning defects, impairing a correct analysis of PGC migration. In wild-type (WT) embryos, at stage 11–12, all PGCs had already migrated to the precursor somatic gonad in the mesoderm and none were found in the pmg (endoderm)

Developmental Biology, Institut de Biologia Molecular de Barcelona, CSIC, Parc Cientific de Barcelona, Baldiri Reixac, 4-8, Barcelona 08028, Spain.

*Author for correspondence (sribmc@ibmb.csic.es)

Received 11 May 2015; Accepted 20 November 2015

Journal of Cell Science

Journal of Cell Science (2016) 129, 354-366 doi:10.1242/jcs.174284

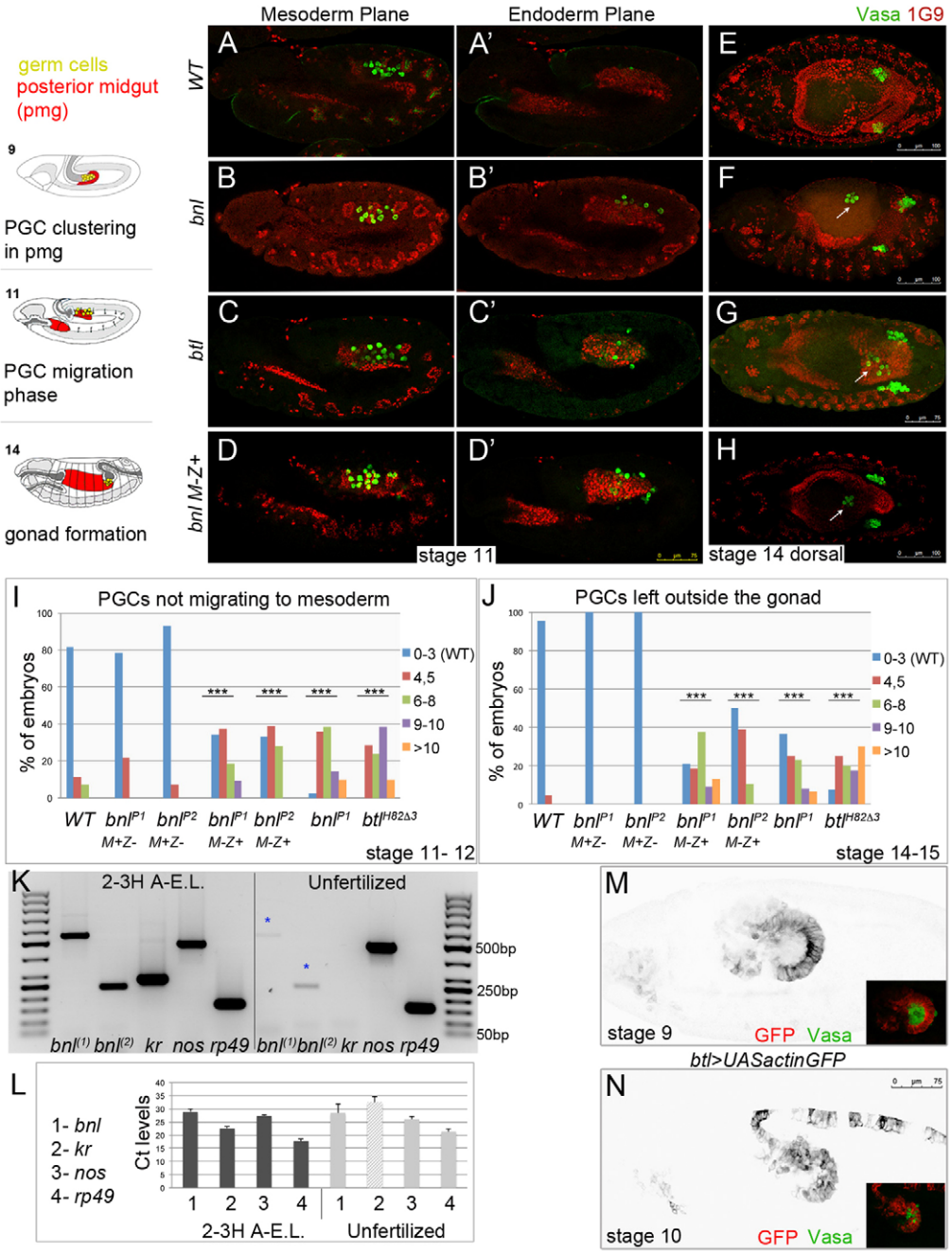

Fig. 1. Bnl–Btl signaling impacts on PGC motility. Confocal single sections of embryos imaged laterally at stage 11–12 (A–D) and dorsally at stage 14 (E–H). Endodermal tissues are labeled with 1G9 (Hindsight) (red) and PGCs are labeled with Vasa (green). A scheme of WT PGC migration at stages 9, 11, 14 is shown on the left. In WT embryos at stage 11–12, all PGCs are already in the mesoderm (A–A′). In bnl^{P1}, $btl^{H82\Delta3}$ and bnl^{P1} *M−Z+* mutant embryos, some PGCs remain attached to the pmg (B′–D′). In WT embryos, all PGCs have migrated to the somatic gonad at stage 14 (E), whereas in bnl^{P1}, $btl^{H82\Delta3}$ and bnl^{P1} *M−Z+* mutant embryos, PGCs are observed on or inside the gut lumen (arrows in F–H). (I,J) Quantification of PGC migration defects. Zero to three PGCs represent WT migration. More than four or five PGCs represent an intermediate migration phenotype, and more than six PGCs outside the gonad represents a strong migration phenotype. (I) *n*=71 (*WT*), 28 (bnl^{P1}*M+Z−*), 28 (bnl^{P2}*M+Z−*), 32 (bnl^{P1}*M−Z+*), 18 (bnl^{21}*M−Z+*), 42 (bnl^{P1}), 21 ($btl^{H82\Delta3}$). (J) *n*=41 (*WT*), 54 (bnl^{P1}*M+Z−*), 44 (bnl^{P2}*M+Z−*), 75 (bnl^{P1}*M−Z+*), 46 (bnl^{P2}*M−Z+*), 60 (bnl^{P1}), 40 ($btl^{H82\Delta3}$). ***P<0.001 (Student's *t*-test). (K,L) Agarose gel of RT-PCR reactions (K) and qRT-PCR amplification (L). In unfertilized eggs, *bnl* is expressed maternally at low level (asterisks) [$bnl^{(1)}$ and $bnl^{(2)}$ represent two different primer pairs, as additional confirmation of expression], the maternal gene *nos* is expressed and *kr*, a zygotic gene, is not detected. *kr* showed no expression in qRT-PCR (no amplification or amplification of less than five cycles as compared to a 'no template' control). All genes are expressed in fertilized embryos, as expected. Data shown for qRT-PCR represent mean±s.e.m. from three independent biological samples and at least three technical replicates [$bnl^{(1)}$ was used for qRT-PCR amplification]. (M,N) Confocal single sections of *btl-GAL4 UASp-Actin5C-GFP* embryos imaged laterally at stages 9 and 10 with *btl* expression in the midgut. Insets are a merge of red (Btl) and green (PGCs) channels, showing the proximity of PGCs to the posterior midgut.

(Fig. 1A,A′,I). In bnl^{P1} and $btl^{H82\Delta3}$ mutant embryos, some PGCs had not migrated and remained adherent to the pmg (Fig. 1B–C′,I). In mutant embryos, ectopic PGCs were not just delayed in migration as indeed many never occupied the gonad, and instead remained in endodermal tissues until after the gonad had been fully formed (Fig. 1E–G,J).

Journal of Cell Science

Journal of Cell Science (2016) 129, 354-366 doi:10.1242/jcs.174284

Surprisingly, we found that *bnl* has a previously unknown maternal function. *bnl* is a haploinsufficient gene, so a phenotype is visible upon loss of 50% its gene function (Sutherland et al., 1996). We took advantage of this genetic property to assess whether the gene had a maternal effect in PGC motility. Embryos laid by mutant mothers crossed to WT males ($bnl^{P1}M-Z+$) showed the same PGC motility defect as bnl^{P1} homozygous mutant embryos, in stark contrast to embryos laid by WT mothers crossed to mutant fathers (bnl^{P1} $M+Z-$), which showed WT PGC migration (Fig. 1D,D′,H–J). To ensure that this was a general property of *bnl* and not specific to this allele, we confirmed this maternal requirement using a second hypomorph allele, bnl^{P2} (Fig. 1I,J). We used bnl^{P1} in all subsequent experiments.

As *bnl* has maternal function, we expected this ligand to be expressed maternally. Analysis of *bnl* expression by *in situ* hybridization (Berkeley Drosophila Genome Project; BDGP) shows that *bnl* is only expressed zygotically. *In situ* hybridization methods do not confidently evaluate small RNA amounts (Semotok et al., 2008), so it is possible that maternal *bnl* expression is present at such low level that it fell below detection. To clarify this point, we measured presence of *bnl* maternal transcripts by quantitative real-time PCR (qRT-PCR), a robust and accurate method for detection of small transcript abundance (Semotok et al., 2008).

In *Drosophila*, maternal RNAs are loaded into the egg and are crucial for early embryonic development until zygotic transcription is initiated; for most genes this occurs at 2.5–3 h after fertilization (De Renzis et al., 2007; Thomsen et al., 2010). To detect maternal *bnl* expression, we used unfertilized eggs laid by WT mothers, in which only maternal RNAs are present. We also analyzed fertilized embryos aged 2–3 h after egg laying, comprising both maternal and newly transcribed zygotic transcripts, to confirm that zygotic *bnl* is present during early embryonic development. We found that *bnl* was expressed maternally at low levels. We used *kr*, one of the earliest expressed purely zygotic gene, as a negative control, *nos*, a bona fide maternal only gene, as a positive control and *rp49* as a loading internal control [*rp49* transcripts are abundant and stable across a 6-h window after egg laying (AEL) both in fertilized and unfertilized eggs]. Using both regular reverse transcriptase PCR and qRT-PCR we detected *bnl* transcripts in samples from unfertilized eggs, whereas *kr* transcripts were not detected (Fig. 1K,L). To make sure that amplification corresponds to cDNA produced from mRNA transcripts and that there was no genomic DNA contamination, we chose primers spanning exon junctions and we ran a control without reverse transcriptase and saw no amplification. We confirmed that *bnl* was expressed zygotically at low levels in this time window.

As bnl^{P2} is a P(LacZ) allele (Sutherland et al., 1996) we further confirmed maternal *bnl* expression by detecting β-gal expression in 1–2 h AEL in bnl^{P2} *P(LacZ)* $M-Z+$ embryos. As expected, we did not detect β-gal signal in embryos in which bnl^{P2} *P(LacZ)* was paternally provided (Fig. S1A,A′). Our results show that *bnl*, besides its zygotic expression and function, is also expressed maternally and has a previously uncovered maternal function. These results are also consistent with RNA-SEQ data from the ModEncode project, which detected unique reads for *bnl* in 0–2 h AEL embryos (ModEncode, FlyBase).

To understand how FGF signaling might affect PGC migration we analyzed where Btl was expressed in correlation to PGCs. We used two different tools: a *btl-Gal4 UASp-Actin5C-GFP* line, which drives GFP under the temporal and spatial pattern of the *btl* gene, and the $btl^{H82\Delta3}$ allele, a P-element lacZ enhancer trap line accurately reflecting Btl expression (Klambt et al., 1992). Both lines showed the same specific expression pattern in the pmg directly adjacent to the cluster of PGCs prior to and during the first stage of migration out of the midgut epithelium (Fig. 1M,N; Fig. S1B,B′) (Shishido et al., 1993).

We conclude that during gastrulation and the initial steps of PGC migration, Bnl signals to its receptor Btl, expressed in the pmg, impacting on PGC movement across this epithelium.

FGF signaling acts in the pmg

Embryos with no maternally provided *bnl* show a strong PGC migration defect. In this genetic background, when we expressed the ligand (*bnl*) or a constitutive form of the receptor (btl^{λ}) using the midgut-specific 48Y-GAL4 line (Fig. S2L,M), we rescued PGC migration (Fig. 2A–D). As Bnl is a secreted ligand there is a less efficient rescue by expression of *bnl* than by expression of btl^{λ}, as expected.

Consistent with a specific requirement of *bnl* and *btl* in the pmg, mesoderm specification or morphogenesis, which would disturb PGC guidance, was not affected in mutant embryos, as both trunk visceral mesoderm and gonadal mesoderm were formed correctly (Fig. S2A–H). Remodeling of the pmg, by delamination of interstitial cell precursors (ICPs) is required for correct PGC motility (Seifert and Lehmann, 2012). To make sure that the PGC motility defect is not due to a pmg cell fate change, we confirmed that the pmg is correctly specified and that ICP cells still delaminate by analyzing inscuteable-lacZ, a lacZ enhancer trap that marks ICP cells (Tepass and Hartenstein, 1995; Kraut and Ortega, 1996), in WT and *bnl* $M-Z+$ embryos (see Fig. S2I,J).

Bnl–Btl signaling is essential for chemoattraction of tracheal cell branches (Klambt et al., 1992; Sutherland et al., 1996). Although tracheal formation and PGC migration have not been linked, the migratory path of the PGCs runs close to tracheal cells and defects in tracheal formation could also account for PGC motility defects. This is not the case because in *trachealess* (*trh*) mutants, in which trachea are not formed, PGC migration was normal [trh^{10512} (n=15) 1.2±1.3 and WT (n=41) 1.2±1 PGCs lost, mean±s.d.].

FGFs have established roles in cell proliferation, cell survival, cell differentiation and cell migration (Muha and Muller, 2013; Wesche et al., 2011). In mammals, these actions are mediated by the mitogen-activated protein kinase (MAPK) or the phosphoinositide 3-kinase (PI3K) pathways and, in some cases, by both pathways (Wesche et al., 2011). In *Drosophila*, FGFs act mostly through the MAPK pathway (Muha and Muller, 2013; Shilo, 2014). Ligand activation of FGFR triggers a Ras–Raf–MEK cassette that ultimately leads to dual phosphorylation and activation of extracellular-signal-regulated kinases (ERKs, Rolled in *Drosophila*). Therefore, presence of dual phosphorylated ERK (dpERK) denotes pathway activation (Gabay et al., 1997).

To determine whether MAPK signaling is active downstream of Btl in the pmg we analyzed dpERK. We observed that, in WT embryos, transient expression of dpERK was restricted to a ventral domain of the pmg epithelia at stage 9 and was lost in *bnl* mutants (Fig. 2E,F). Overexpression of btl^{λ} or *bnl* in the midgut in *bnl* mutant embryos led to re-activation of dpERK (Fig. 2G,H). These results suggest that dpERK expression in the pmg is dependent on *bnl* and *btl*.

Taken together our results indicate that Bnl–Btl signaling is required specifically in the pmg epithelium for correct PGC motility.

FGF signaling modulates E-cadherin clustering

The invaginating pmg forms an adhesive cable around the cells that is maintained as long as cells stay epithelial (Tepass, 1996; Tepass and Hartenstein, 1994). The adhesive cable is formed by accumulation of

Journal of Cell Science (2016) 129, 354-366 doi:10.1242/jcs.174284

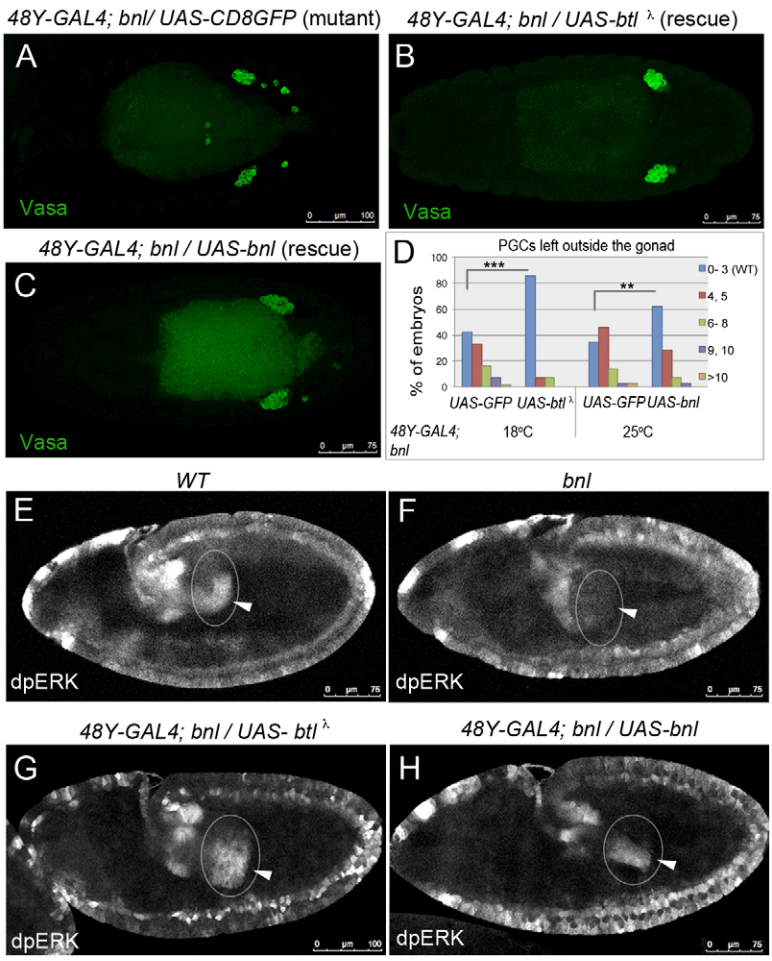

Fig. 2. FGF signaling in midgut epithelia is required for PGC motility. (A–C) Confocal projections of embryos imaged dorsally at stage 14, labeled with Vasa. *48Y-Gal4; bnl^{P1}/UAS-CD8GFP* mutant embryos show PGCs that have not correctly migrated (A). When *bnl or btl$^{\lambda}$* are added back in the pmg, PGC migration is rescued (B,C). (D) Quantification of PGC migration defects at stage 14 (*n* values, 18°C control=55, *UAS-btl$^{\lambda}$*=28, 25°C control=35, *UAS-bnl*=42). *48Y-Gal4; bnl^{P1}/UAS-btl$^{\lambda}$* embryos show patterning defects at 25°C, so this experiment was carried out at 18°C. ***P*<0.01; ****P*<0.001 (Student's *t*-test). Two different lines of UAS-*btl$^{\lambda}$* showed the same results but only results with the line on chromosome II are shown. (E–H) Confocal single sections of embryos imaged laterally at stage 9, labeled for dpERK. In WT embryos, the dpERK signal is observed ventrally at the blind end of the pmg (arrowhead in E). This expression is absent in *bnl^{P1}* mutant embryos (arrowhead in F). Overexpression of *btl$^{\lambda}$* or *bnl* in the pmg in the mutant background restores the dpERK signal (arrowheads in G,H). Circles indicate the whole pmg area.

E-cadherin and other adherens junction components at the membrane. Adherens junction protein accumulation in epithelia leads to stronger cell adhesion and, in concert with the actin cytoskeleton, would confer the tissue strength required for the dynamic morphogenetic movements of pmg formation (Adams and Nelson, 1998; Maitre and Heisenberg, 2013).

In WT embryos, the pmg forms a perfect cable and E-cadherin is clustered evenly at the junctional belt (Fig. 3A,C). We observed that in *bnl M−Z+* embryos, the adhesive cable was disrupted from the point of its formation, and pmg cells presented uneven borders, suggestive of reduced tissue tension (Lecuit and Lenne, 2007) (Fig. 3B). We reasoned that FGF might regulate E-cadherin distribution in the pmg. Indeed, by stage 9, during pmg extension, in *bnl M−Z+* mutants, and *bnl* and *btl* mutants E-cadherin was not clustered at adherens junctions and embryos showed breakage of the adherens junction adhesive cable at the blind end of the pmg pocket, in the domain of FGF activation (Fig. 3D–G). As increased cell death in the pmg tissue could account for these tissue shape changes we confirmed by terminal deoxynucleotidyl transferase dUTP nick end labeling (TUNEL) staining in mutant embryos that there was no cell death in the pmg (Fig. S3A,D).

Armadillo (Arm; the *Drosophila* β-Catenin) is one of E-cadherin-binding partners and is also concentrated at adherens junctions, being transported together with E-cadherin through the biosynthetic pathway (Langevin et al., 2005). We reasoned that if FGF is required for E-cadherin clustering, Arm localization should also be affected. Indeed, we found that Arm in *bnl M−Z+* mutants was not clustered at the adhesive belt, as observed for E-cadherin (Fig. S3E,F).

Our data indicate that FGF signaling modulates E-cadherin localization or maintenance at adherens junctions in the pmg epithelium.

FGF signaling modulates distribution of zygotic E-cadherin

E-cadherin distribution at mature adherens junctions, in tissues undergoing morphogenetic movements, is due primarily to endocytosis and recycling (Wirtz-Peitz and Zallen, 2009). The small Rab GTPases are crucial regulators of protein trafficking, including that of E-cadherin (Wirtz-Peitz and Zallen, 2009; Zerial and McBride, 2001). Rab5 is required for E-cadherin internalization into early endosomes and transport to lysosomal degradation and Rab11 regulates recycling to the plasma membrane (Kamei et al., 1999; Langevin et al., 2005; Le et al., 1999; Lock and Stow, 2005; Palacios et al., 2005). Rab11 is also responsible for transport of newly synthesized proteins to the plasma membrane, and at least in mammalian cells, for targeting of newly made E-cadherin (Desclozeaux et al., 2008; Lock and Stow, 2005).

To assess whether defective E-cadherin trafficking could account for E-cadherin misdistribution in the pmg we analyzed embryos expressing dominant-negative forms of Rab5 and Rab11 (Rab5^{DN} and Rab11^{DN}), which have been shown to accurately reflect Rab loss of function (Satoh et al., 2005; Shimizu et al., 2003), in the pmg epithelium. Surprisingly, expression of Rab11^{DN} in the pmg led to disruption of E-cadherin clustering with breakage of the adhesive belt, which is very similar to that observed upon loss of *bnl* and *btl*, whereas expression of Rab5^{DN} showed no such defects (Fig. 4B,C,E). Shibire (the *Drosophila* Dynamin) is essential for clathrin-mediated

Journal of Cell Science

Journal of Cell Science (2016) 129, 354-366 doi:10.1242/jcs.174284

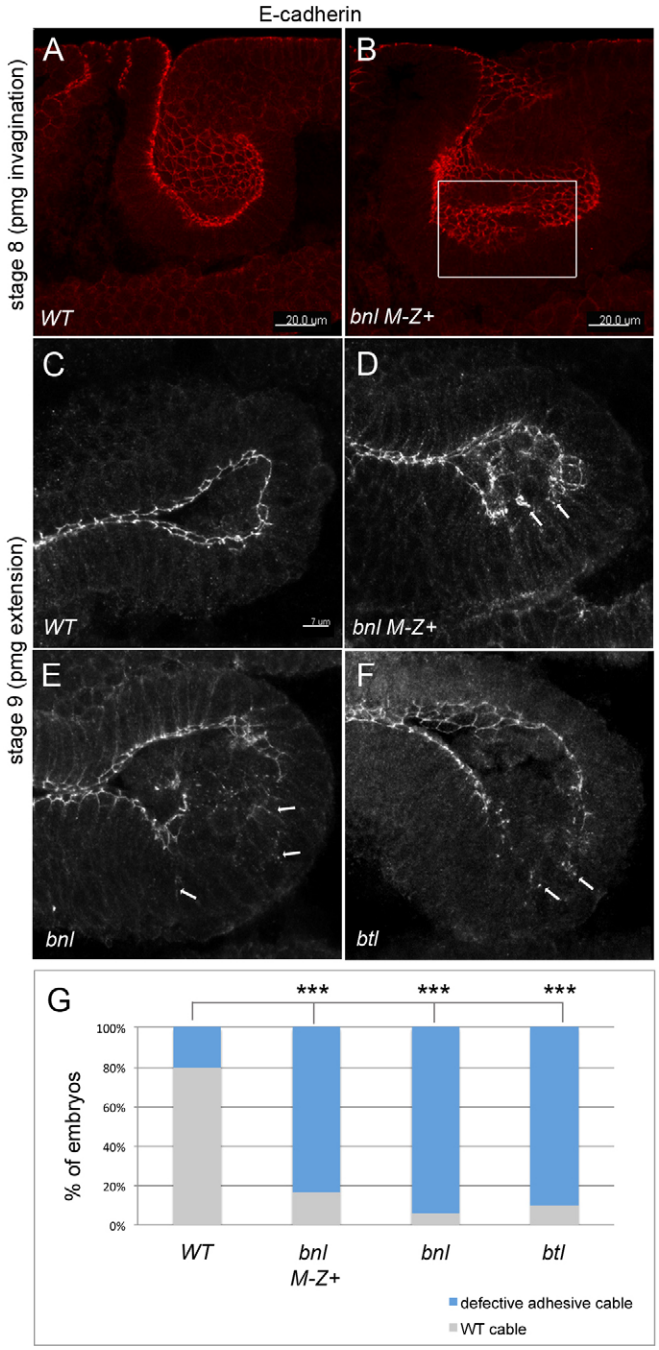

Fig. 3. FGF signaling modulates E-cadherin clustering at the adhesive belt. (A,B) 2-µm stacks of embryos imaged laterally at stage 8, labeled with E-cadherin. In *bnl M–Z+* mutant embryos, the pmg adhesive cable is already broken (B, box). (C–F) 4-µm stacks of embryos imaged laterally at stage 9, labeled with E-cadherin. In WT embryos the pmg adhesive cable is intact (C). In *bnl M–Z+*, *bnl* and *btl* mutant embryos, E-cadherin is not correctly clustered in spots at adherens junctions (arrows) and the adhesive cable is broken at the blind end of the pmg. (G) Quantification of phenotype (*n* values, *WT*=15, bnl^{M-Z+}=18, *bnl*=17, *btl*=10). ***P<0.001 (χ^2 test).

endocytosis. As additional confirmation that defects in E-cadherin endocytosis are not responsible specifically for E-cadherin misdistribution at adherens junctions we analyzed embryos expressing $shibire^{DN}$ (shi^{DN}) in the pmg and found that both E-cadherin distribution and cable formation were normal (Fig. 4D,E). Importantly, as with pmg defects caused by *bnl* and *btl*, PGCs did not migrate correctly in $Rab11^{DN}$-expressing embryos, whereas no migration defect was observed when $Rab5^{DN}$ was expressed in the pmg (Fig. 4F). These results further show the impact of pmg epithelial morphogenesis on PGC motility. Our data suggest that FGF signaling acts on recycling of E-cadherin to plasma membrane or along the E-cadherin biosynthetic pathway.

Zygotic E-cadherin is required, together with maternally provided E-cadherin, in dynamic epithelia undergoing morphogenetic movements that require stronger cell adhesion to withstand mechanical forces. In the absence of zygotic E-cadherin, static epithelia are not affected, being able to rely only on maternal E-cadherin. However, in dynamic epithelia loss of zygotic E-cadherin causes loss of tissue integrity, even in the presence of maternal protein (Tepass et al., 1996; Uemura et al., 1996). We hypothesized that zygotic E-cadherin could also be essential for pmg morphogenesis and that, in FGF mutants, zygotic E-cadherin would not be correctly targeted, affecting tissue integrity.

To evaluate the contribution of maternal and zygotic E-cadherin expression during *Drosophila* gastrulation, and specifically during pmg morphogenesis, we used a knock-in allele of *E-cadherin*, *DE-cad::GFP*, obtained through insertion of E-cadherin-GFP into the gene locus fully recapitulating E-cadherin expression (Huang et al., 2009). To visualize maternal expression we analyzed embryos from *DE-cad::GFP* (i.e. expressing GPF-tagged E-cadherin) females crossed to WT males. Conversely, we tested zygotic expression by analyzing embryos from *DE-cad::GFP* males crossed to WT females. We found that, during pmg invagination, E-cadherin was already visible in the embryonic ectoderm although not yet as stably localized at the adherens junctions as with the maternally loaded protein (Fig. 5A,B). Interestingly, at this stage, zygotic E-cadherin levels were higher in the invaginating pmg, contributing significantly to the total E-cadherin at the adhesive cable (Fig. 5A′,B′). We found that this zygotic E-cadherin at the adhesive cable was mislocalized in *bnl* mutants. We used the same experimental rationale and crossed *DE-cad::GFP* males with either *bnl* or WT females. In *bnl* mutants, zygotic E-cadherin was not clustered at the adhesive cable and was observed instead around the cell (Fig. 5D).

To demonstrate that in FGF mutants only targeting or turnover of zygotic, and not maternal, E-cadherin is affected, we directly compared the total E-cadherin signal with the signal originating only from zygotic E-cadherin. We detected endogenous and newly expressed E-cadherin by using an antibody against the protein (maternal and zygotic; anti-DE-CAD2 antibody), and only zygotic protein by expressing a functional DE-cadherin–GFP fusion protein (Oda and Tsukita, 1999) uniformly from the time of gastrulation using nullo-GAL4, which was detected with an anti-GFP antibody. Importantly, the anti-DE-CAD2 and anti-GFP antibodies recognize different parts of DE-cadherin–GFP (Oda and Tsukita, 1999). Using this assay, we found, as expected, that in WT embryos the two markers colocalized at the adhesive cable, indicating that zygotic E-cadherin is correctly targeted (Fig. 5E–E″).

Interestingly, in *bnl M–Z+* mutants zygotic E-cadherin was not clustered at the adhesive cable, as visualized by the GFP signal, and instead localized within the cell and at basolateral membranes (Fig. 5F,F″). Consistent with our hypothesis, maternal E-cadherin was correctly clustered, as detected with anti-E-cadherin antibody (Fig. 5F,F′).

We propose that Bnl–Btl signaling regulates, directly or indirectly, Rab11-dependent targeting and/or turnover of zygotic E-cadherin on pmg epithelial cells. We further suggest that zygotic E-cadherin is needed, together with maternally provided E-cadherin, in the pmg to

Journal of Cell Science

Journal of Cell Science (2016) 129, 354-366 doi:10.1242/jcs.174284

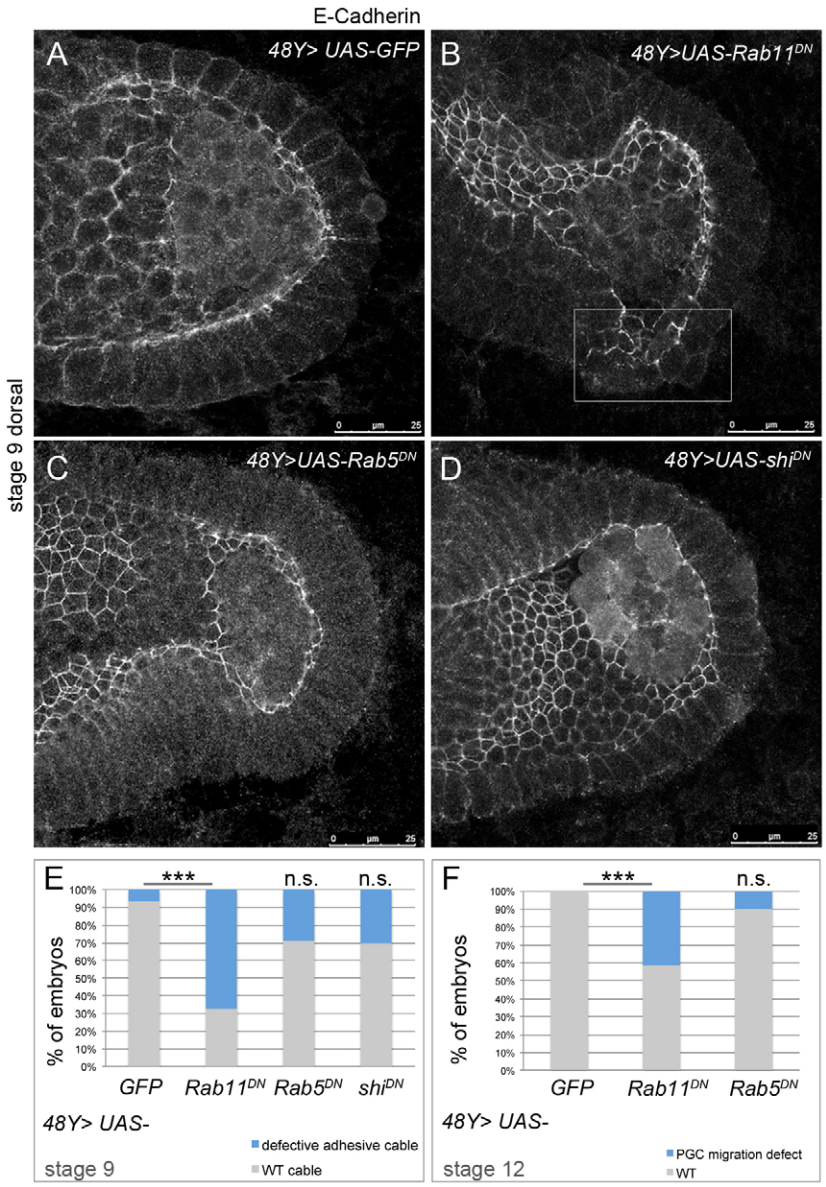

Fig. 4. E-cadherin localization at the adhesive cable is Rab11 dependent. (A–D) Confocal single sections of embryos imaged dorsally at stage 9, labeled with E-cadherin. In 48Y>UAS-GFP (WT) (A), *48Y>UAS-Rab5^{DN}* (C) and *48Y>UAS-shi^{DN}* (D) embryos, the pmg adhesive cable is intact. In *48Y>UAS-Rab11^{DN}* embryos (B) E-cadherin is not correctly clustered and the adhesive cable is broken, phenocopying *bnl M−Z+*, *bnl* and *btl* mutant phenotype. The box shows the defective pmg area. (E,F) Quantification of the pmg phenotype (*Rab11^{DN}*, 67.57%±5.89; *Rab5^{DN}*, 28.88%±12.24; *shi^{DN}*, 29.28%± 0.69; mean±s.d.; *n* values, *WT*=15, *Rab11^{DN}*=37, *Rab5^{DN}*=45, *shi^{DN}*=20) (E) and PGC migration phenotype at stage 12 (*Rab11^{DN}*, 40%±19.13; *Rab5^{DN}*, 10%±4.77; mean ±s.d.; *n* values, WT=35, *Rab11^{DN}*=60, *Rab5^{DN}*=71) (F). ***P<0.001 (χ^2 test).

make the adhesive belt that confers strength to the dynamic process of gut morphogenesis, maintaining epithelium integrity.

FGF-dependent midgut pocket formation regulates PGC clustering and motility

Our observation that PGCs remained adhered to the pmg in FGF mutants seemed counterintuitive with a role of FGF signaling in maintenance of cell adhesion. We therefore sought to understand the requirement of FGF signaling in the pmg epithelium that specifically impairs PGC motility. Since their formation, PGCs are at all times in close association with pmg precursor cells. At stage 9, the pmg lumen forms a characteristic pocket carrying clustered PGCs that show little contact with surrounding pmg cells (Kunwar et al., 2008) (Figs 3C, 6D; Movie 1). PGCs migrate through the pmg epithelium at stage 10, taking advantage of spaces created during midgut transition from epithelia to mesenchyme (Seifert and Lehmann, 2012). In *bnl M−Z+*, *bnl* and *btl* mutant embryos, PGCs do not cluster and instead disperse in the midgut lumen [82% of *bnl M−Z+* embryos (n=22), as compared to 0% in WT embryos (n=12) with significance of P<0.001 by χ^2 test] (Fig. 6E–G). PGC clustering is likely aided by the morphogenetic events that lead to midgut lumen formation because in WT embryos, during pmg invagination, PGCs were tightly packed in the midgut pit (Fig. 6A). In contrast, in *bnl M−Z+* embryos, the midgut pocket was deformed, not forming the characteristic pit and PGCs were already dispersed (Fig. 6B).

The pmg epithelium undergoes dynamic cell shape changes during invagination and extension for reorganization of midgut epithelial cells and pocket formation (Sweeton et al., 1991; Tepass, 1996). *bnl* and *btl* mutant embryos show normal pmg invagination, a process that depends on cell apical constriction and recruitment of Myosin II (Costa et al., 1994; Pilot and Lecuit, 2005; Sweeton et al., 1991). To investigate the pmg defect in mutants, we performed 3D reconstructions during pmg extension, at stage 9, using E-cadherin as a marker of apical epithelial surfaces. Consistent with the defect observed at stage 8, in *bnl M−Z+*, *bnl* and *btl* mutants, although the gut had extended, we found that the midgut tissue did not zip anteriorly (arrows, Fig. 6F,G), and the pocket, with its characteristic concave curvature was not properly formed (see Movie 1). As a result, PGCs were unable to cluster

Journal of Cell Science

Journal of Cell Science (2016) 129, 354-366 doi:10.1242/jcs.174284

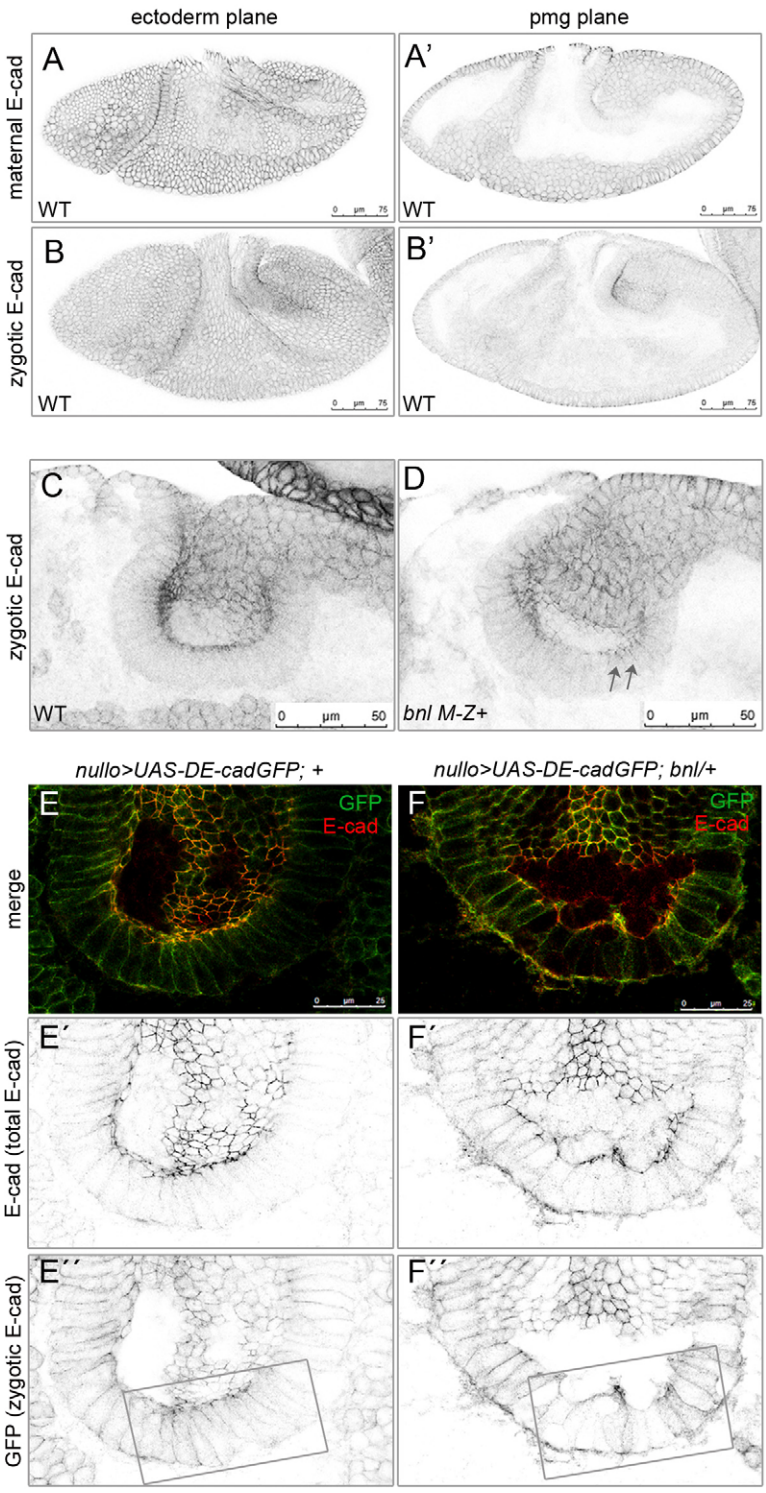

Fig. 5. FGF signaling modulates targeting of zygotic E-cadherin. (A,B) Confocal single sections of WT embryos imaged laterally at stage 7, at two different planes. (A) Maternal E-cadherin detected by anti-GFP antibody in embryos of *DE-cad::GFP* females crossed to WT males. (B) Zygotic E-cadherin detected by anti-GFP antibody in embryos of WT females crossed to *DE-cad::GFP* males. Images were collected using the same settings to allow signal comparison. (C,D) Confocal single sections of embryos from WT (C) or *bnl* (D) females crossed to *DE-cad::GFP* males imaged laterally at stage 9. Embryos are labeled with GFP to visualize zygotic E-cadherin. In *bnl M−Z+* embryos zygotic E-cadherin is observed at basolateral membranes (arrows) and not clustered at adherens junctions. (E–F″) Confocal single sections of WT (E) or *bnl M−Z+* (F) embryos, imaged dorsally, highlighting the pmg and expressing zygotic *DE-cadGFP* uniformly in the embryo, using *nullo-GAL4*. Embryos were labeled with E-cadherin (red) and GFP (green) to reveal, respectively, total E-cadherin protein and zygotic E-cadherin. In *bnl M−Z+* embryos, zygotic E-cadherin is not correctly clustered at the adhesive cable (F″). Boxes indicate affected area.

within this pocket and dispersed anteriorly within the midgut tissue (arrowheads, Fig. 6E–G).

As our data suggests that Bnl and Btl signaling regulates targeting and/or turnover of zygotic E-cadherin in pmg epithelial cells, we expected the same pmg defect in *shg* zygotic mutants. Indeed, we found that *shg* zygotic mutants have pmg shape defects similar to those in *bnl* and *btl* mutants (Fig. 6H; Movie 1).

To investigate further this tissue shape defect, we imaged WT and *bnl M−Z+* embryos that also carried *DE-cad::GFP*. Consistent with the role of Bnl and Btl in E-cadherin targeting, in mutant embryos the epithelium was cuboidal, suggestive of lower intracellular adhesion (Fig. 6J). Moreover, in *bnl M−Z+* mutants, although a lumen was present, the round cavity where PGCs normally lie had collapsed and had a characteristic elongated form with PGCs trapped ectopically in tissue folds in anterior and dorsal regions of the pmg (Fig. 6I,J; Fig. S4A,B).

After PGC clustering in the pmg pocket, midgut remodeling, through delamination of interstitial cell precursors (ICP) from the midgut epithelia, is required for PGC transepithelial movement (Seifert and Lehmann, 2012; Tepass and Hartenstein, 1995). We

Journal of Cell Science

Journal of Cell Science (2016) 129, 354-366 doi:10.1242/jcs.174284

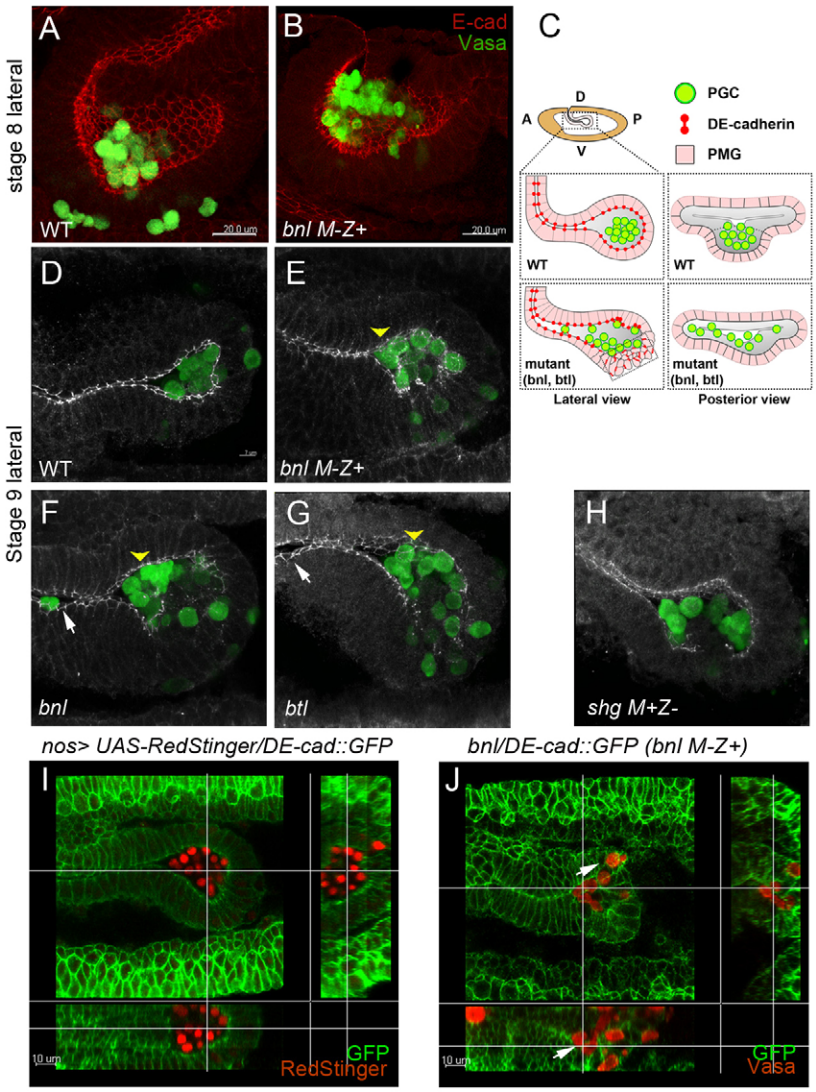

Fig. 6. FGF dependent midgut pocket formation regulates PGC clustering. (A,B) 2-µm stacks of embryos imaged laterally at stage 8. PGCs are labeled with Vasa (green), and pmg epithelium labeled with E-cadherin (red). In WT embryos, the pmg forms a depression (pit) that accommodates the PGC cluster (A). In *bnl M−Z+* embryos the pmg does not form a pit and PGCs disperse anteriorly and dorsally (B). (C) Scheme showing WT and mutant pmg shape and PGC localization from a lateral and posterior view at stage 9. (D–H) 4-µm stacks of embryos imaged laterally at stage 9. PGCs labeled with Vasa (green) and pmg epithelium labeled with E-cadherin (gray). In WT embryos the pmg epithelium is closed anteriorly and the midgut pocket is concave allowing the formation of a round cavity at its blind end, where PGCs lie (D). In *bnl M−Z+*, *bnl* and *btl* mutant embryos the midgut tissue does not zip anteriorly (arrows in E–G) and the pocket is not properly shaped resulting in dispersion of PGCs anteriorly within the pmg tissue (arrowheads in E–G). pmg defects were observed in 9/10 embryos for *bnl M−Z+*, 7/9 for *bnl* and 6/6 for *btl*. *shg M+Z−* mutants have similar pmg shape defects (H). For a 3D reconstruction of embryos D–H, see Movie 1. Embryos and images shown in D–G are the same as in Fig. 3C–F, but including the green (PGC) channel, to be able to directly compare and correlate the two phenotypes (pmg defects and PGC motility). (I,J) Orthogonal views of *nos>RedStinger/DE-cad::GFP* (*WT*) and *bnl/DE-cad::GFP* (*bnl M−Z+*) embryos imaged laterally at stage 9, labeled with GFP (E-cadherin) (green), and RedStinger (nuclear version of DsRed) or Vasa (red) (to mark PGCs). In WT embryos, all PGCs are clustered inside the pmg lumen cavity (I), whereas in mutant embryos some PGCs are trapped in anterior and dorsal areas of the defective pmg (arrows in J).

could clearly see that, in WT embryos, ICP delamination occurred before a complete loss of pmg epithelial characteristics, representative of EMT, and that PGCs crossed the epithelia at this time (Fig. 7A,B). In *bnl M−Z+* embryos, ICP cells still delaminated (Fig. 7C) but some PGCs had dispersed and remained adherent to more anterior regions of the pmg, closer to the hindgut (Fig. 7D).

Moreover, we observed that in late stage 10 WT embryos, after EMT and PGC transepithelial movement had proceeded, some E-cadherin was still present in anterior regions of the midgut both in WT and *bnl M−Z+* embryos and that ectopically located PGCs remained adherent to this region in mutant embryos (Fig. 7E,F,H). To demonstrate that these PGCs were indeed adhesive, we reduced E-cadherin, encoded by *shg*, in the embryo in a *bnl M−Z+* background (*shg/+; bnl/+*) and observed that ectopic PGC adhesion was released (Fig. 7G,H).

Our data indicates that in the absence of FGF signaling the pmg pocket collapses, likely as a result of lower cell–cell adhesion, and that ectopic pmg cell–cell adhesions are created anteriorly. As a consequence PGC movement is impaired due to PGC dispersion into more adhesive anterior regions, outside of the FGF domain of action, and trapping of PGCs in tissue folds. We conclude that FGF signaling is required at the blind end of the pmg for correct adhesive cable formation and maintenance of the 3D tissue architecture, allowing PGC clustering and subsequent movement.

FGF signaling regulates epithelial integrity

Our results suggest that the role of FGF signaling on targeting of zygotic E-cadherin contributes to maintenance of the pmg epithelial integrity (Fig. S4C–F). As Btl is expressed in endodermal and ectodermal tissues, we reasoned that Bnl–Btl signaling could be required more globally in other Btl-expressing epithelia. To determine whether loss of Btl signaling is sufficient to induce loss of cell adhesion, we used a tissue that has endogenous Btl expression and in which lack of cell adhesion would be easily seen through the appearance of tissue gaps: the ventral midline. The ventral midline is composed of two rows of mesectodermal cells that are integrated as epithelial cells in the surface ventral ectoderm of the embryo until stage 12 of embryogenesis. We expressed GFP together with a dominant-negative form of *btl* (btl^{DN}) in epidermal stripes of three or four cells per segment, using *engrailed–gal4* (*en-GAL4*) (Fig. 8A). To simultaneously create a *btl*-sensitized background and visualize *btl* expression, the btl^{DN} line also carried the $btl^{H82\Delta3}$ lacZ enhancer trap allele. *en-GAL4* was chosen as a driver to induce *btl* loss of function in stripes so that the neighboring stripes could be used as a

Journal of Cell Science (2016) 129, 354-366 doi:10.1242/jcs.174284

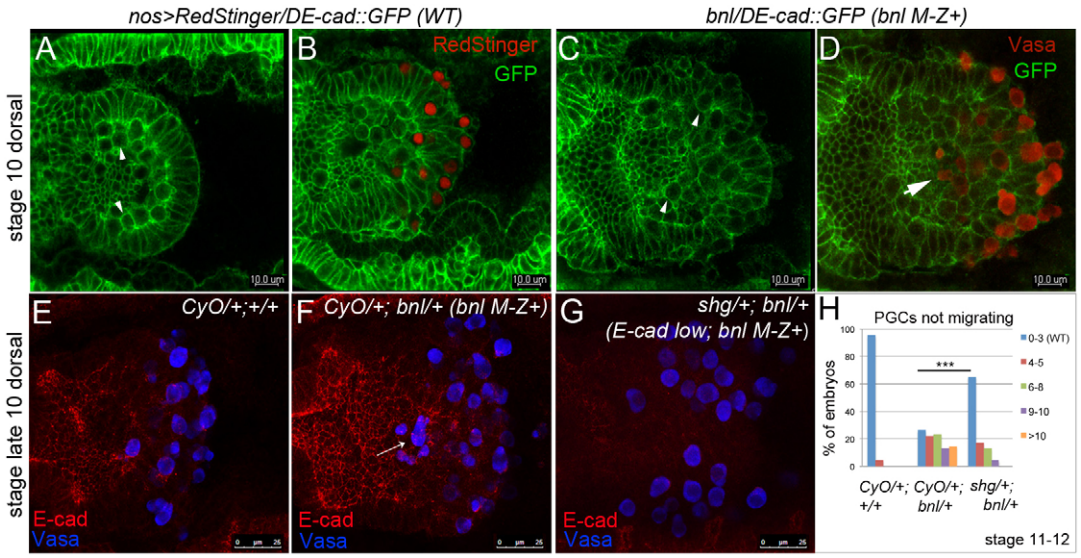

Fig. 7. FGF-dependent PGC clustering aids PGC motility. (A–D) Single confocal sections of *nos-GAL4>RedStinger/DE-cad::GFP* (WT) (A,B) and *bnl/DE-cad::GFP* (*bnl M–Z+*) (C,D) embryos imaged dorsally at stage 10 (during PGC transepithelial migration), at two different planes (A,C, deeper; B,D, 5–10 µm above that shown in A,C). E-cadherin in epithelia is labeled with GFP (green), and PGCs are labeled with RedStinger (B) or Vasa (D) (red). In WT embryos, ICP cells delaminate before EMT occurs (arrowheads in A) and PGC migrate at this time (B). In *bnl M–Z+* embryos, ICP cells still delaminate (arrowheads in C) but some PGCs remain adherent anteriorly (arrow in D). (E–G) Confocal projections of embryos imaged dorsally at late stage 10. In control embryos, after EMT, the pmg still shows high E-cadherin in more anterior regions (E). In *bnl M–Z+* embryos, ectopic PGCs remain adherent those areas (arrow in F). Reducing zygotic *shg* lowers overall E-cadherin levels and frees PGCs (G). (H) Quantification of PGC migration phenotype at stage 11–12 (*n* values, *CyO/+;+/+*=64, *CyO/+;bnl/+*=76; *shg/+;bnl/+*=46). ***P<0.001 (Student's *t*-test).

control. We found that *btl* loss of function leads to lower tissue adhesion. In stripes where btl^{DN} is expressed, as visualized by GFP expression, we observed the appearance of tissue gaps (Fig. 8B). Loss of tissue adhesion is specific to loss of Btl signaling and is not a cellular artifact, as we only observed it upon expression of btl^{DN} (Fig. 8D) and not with GFP alone (Fig. 8C).

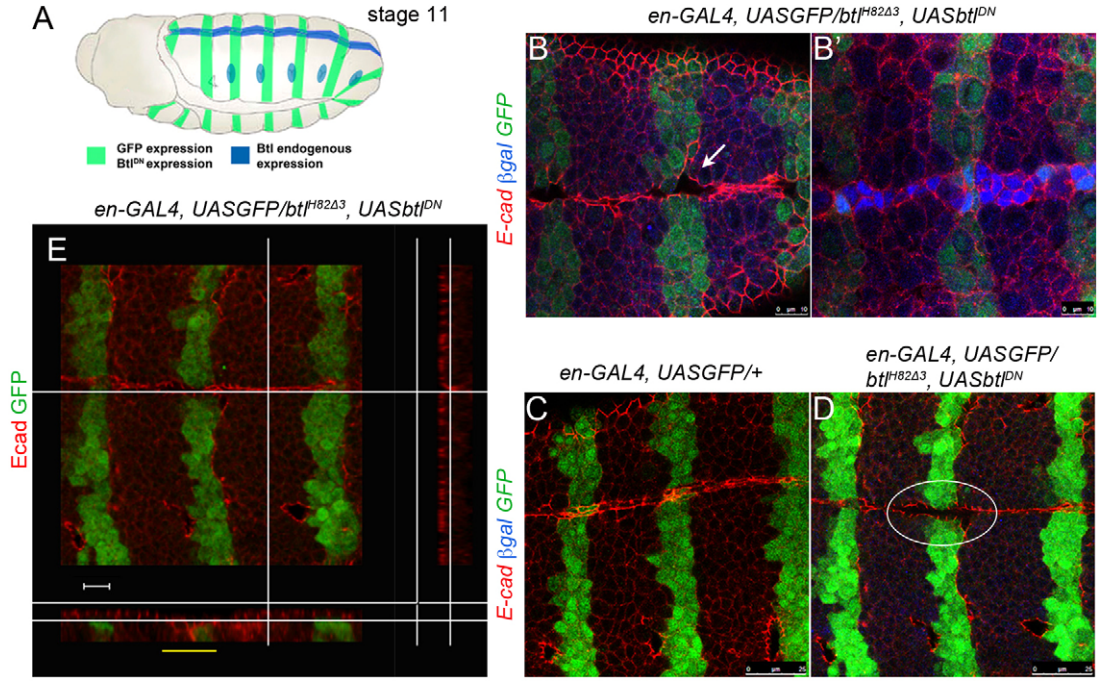

Fig. 8. FGF signaling maintains epithelial integrity. (A) Experimental scheme. (B–B′) Two confocal planes of *en-GAL4, UASGFP/*$btl^{H82\Delta3}$*, UASbtl*^{DN} embryos imaged ventrally in the ectoderm at stage 11, labeled with E-cadherin (red), β-Gal (Btl expression in blue) and GFP (green). Expression of btl^{DN} in stripes leads to loss of cell–cell adhesion in midline cells (arrow in B), where Btl is expressed (blue in B′). (C,D) Confocal single sections of *en-GAL4, UASGFP/+* and *en-GAL4, UASGFP/*$btl^{H82\Delta3}$*, UASbtl*^{DN} embryos imaged ventrally, labeled with E-cadherin (red), β-Gal (blue) and GFP (green). Loss of cell adhesion is only observed when btl^{DN} is expressed (circle). (E) Orthogonal view of an *en-GAL4, UASGFP/*$btl^{H82\Delta3}$*, UASbtl*^{DN} embryo showing cell rounding in areas of btl^{DN} expression (yellow line). Scale bar: 10 µm.

Journal of Cell Science

Journal of Cell Science (2016) 129, 354-366 doi:10.1242/jcs.174284

We expected that cell rounding would accompany this loss of cell adhesion. To test this prediction we made transversal images of cells in embryos expressing btl^{DN}. We saw that mutant cells (within the GFP stripe) showed cell rounding and uniform E-cadherin in contrast to cells not expressing btl^{DN} (Fig. 8E).

We conclude that FGF signaling, through Bnl and Btl, has a role in maintenance of epithelial integrity in endodermal and ectodermal tissues, where Btl is expressed.

DISCUSSION

Maintenance of cell adhesion is crucial during morphogenesis where E-cadherin plays an essential role. A basal level of E-cadherin is required for all embryonic development, whereas active epithelia require stronger bonds and increased E-cadherin at adherens junctions. In *Drosophila*, this is achieved by the presence of both zygotic and maternal E-cadherin. Here, we propose that Bnl–Btl signaling is required for correct targeting or turnover of zygotic E-cadherin. We suggest that FGF-dependent targeting of zygotic E-cadherin to the adhesive cable is needed for pmg pocket integrity, as reliance only on maternal E-cadherin is not sufficient to withstand the forces involved in morphogenesis, leading to pocket collapse. We show that pmg pocket collapse, in turn, has strong repercussions for PGC movement, uncovering another level of adhesion regulation for PGC motility, in addition to adhesion regulation through peroxiredoxin signaling (DeGennaro et al., 2011) and midgut remodeling (Seifert and Lehmann, 2012). Our findings also highlight the necessity for coordinated cell shape changes and adhesion regulation in different cell types during embryo development.

bnl was thought to be only expressed zygotically and its functions have been mostly analyzed in the context of tracheal cell migration at later embryonic stages. We show that *bnl* is also expressed maternally and has a previously unappreciated maternal effect function in early *Drosophila* development. We find that embryos from *bnl* females crossed to WT males (*bnl M−Z+*) have defective pmg morphogenesis, impacting on PGC migration, whereas embryos from *bnl* males crossed to WT females (*bnl M+Z−*) show no defects. In animals, the maternal genome controls most of early embryonic development as zygotic transcription and concomitant maternal transcript degradation occurs only after the first developmental stages, leading to a shift of biological functions over to the zygotic genome. In *Drosophila*, this transition occurs at 2–3 h AEL, just before the time of pmg morphogenesis, and when we first observe a requirement for Bnl–Btl signaling (i.e. during stages 6–9, 3–4.30 h AEL) both ligand and receptor need to be present and functional. Btl is expressed zygotically from stage 5 and is localized at the anterior and posterior midgut primordium (Klambt et al., 1992; Shishido et al., 1993). At these stages, Bnl is expressed zygotically at low levels (BDGP, Fig. 1K,L) and our data suggests that it relies on its maternal transcripts to perform these early functions.

We show that in *bnl* and *btl* mutants the pmg can invaginate and extend but, as the tissue is now likely solely dependent on maternal E-cadherin, it has weaker cell adhesions and a resulting cuboidal epithelium (Figs 3, 5 and 6). FGF has a clear role as a chemoattractant in tracheal migration (Muha and Muller, 2013; Sutherland et al., 1996). We show a new role in maintenance of epithelial integrity and tissue architecture through modulation of zygotic E-cadherin distribution.

What defines these two different outputs of FGF signaling? It has been suggested that activation of FGFR with high levels of FGF ligand would promote cell–cell contacts and a lower level of ligand would promote chemoattraction (Bae et al., 2012). Although this is an attractive hypothesis, our data does not allow us to conclude how FGF levels could promote each output. We could also envision that a uniform signal promotes cell–cell contacts, whereas a localized signal promotes chemoattraction because in tracheal development localized Bnl is needed for chemoattraction of tracheal branches (Sutherland et al., 1996). This would be consistent with our data, as when we express constitutively active Btl in the whole midgut, we rescue the pmg morphogenesis defect, suggesting that localized Btl activity is not necessary. These two hypotheses are, however, not mutually exclusive.

Interestingly, our data suggests that FGF signaling modulates zygotic E-cadherin through targeting or turnover to mature adherens junctions. Using an assay that simultaneously visualizes total E-cadherin and only zygotic E-cadherin, we showed that only zygotic E-cadherin is mis-targeted in FGF signaling mutants (Fig. 5). There are a wealth of studies on regulation of E-cadherin dynamics at the plasma membrane but there is little evidence for a direct role of Rab proteins on E-cadherin trafficking and particularly how E-cadherin is routed and trafficked to the plasma membrane. Moreover, there is only one study on E-cadherin trafficking in *Drosophila*. The colocalization of E-cadherin and recycling endosomes has been reported in *Drosophila* pupal epithelia, but a requirement for Rab11 for E-cadherin distribution was not investigated and neither was whether this E-cadherin was rerouted or newly synthesized (Langevin et al., 2005). In MDCK and HeLa cells, trafficking of newly made E-cadherin goes through Rab11-positive recycling endosomes from the Golgi to the plasma membrane (Desclozeaux et al., 2008; Lock and Stow, 2005). In MDCK cells, overexpression of a dominant-negative form of Rab11 leads to sequestration of E-cadherin in recycling endosomes (Lock and Stow, 2005). When we overexpressed $Rab11^{DN}$ in the pmg epithelia, we prevented E-cadherin accumulation at the adherens junctions in the plasma membrane, suggesting that in *Drosophila* epithelia trafficking of E-cadherin is also achieved through Rab11-positive recycling endosomes. Moreover, expression of $Rab11^{DN}$ phenocopies the distribution and adhesive cable disruption observed in FGF mutants (Fig. 4), suggesting that FGF signaling functions in trafficking of E-cadherin through recycling endosomes.

Expression of dominant-negative forms of Rab5 or Shibire in the posterior midgut does not prevent E-cadherin accumulation at adherens junctions. This suggests that at early stages of pmg morphogenesis there is not a strong requirement for turnover of E-cadherin to and from the plasma membrane, a function that would likely require internalization through clathrin vesicles into Rab5-positive early endosomes. Considering the nature of the dominant-negative constructs that could express at different times and levels at this stage or in this tissue, we cannot fully rule out a role for endocytosis in pmg morphogenesis. Nevertheless, our data is consistent with a predominant requirement for targeting or recycling of zygotic E-cadherin during pmg adhesive cable formation with a minor role being played by the endocytic machinery.

We still do not know how mechanistically FGF signaling modulates E-cadherin distribution and whether this role is direct or indirect. This would be an interesting avenue of research. It has been reported, in migratory border cells, that Pvr signaling, through the small GTPase Rac, increases recycling endosome levels (Wan et al., 2013), leading presumably to increased E-cadherin transport to adherens junctions. By contrast, in tracheal cells, Rac functions to maintain lower E-cadherin levels and it has been suggested that Btl–Bnl signaling activates Rac as these two signaling pathways genetically interact (Chihara et al., 2003). Thus, RTK signaling

Journal of Cell Science (2016) 129, 354-366 doi:10.1242/jcs.174284

could regulate, positively or negatively, Rac activity, which in turn would be necessary to maintain the levels of recycling endosomes transporting E-cadherin to adherens junctions. FGF signaling could also have an indirect role on Rab11-dependent E-cadherin trafficking through its impact on the actin cytoskeleton. It has been shown that E-cadherin trafficking to the plasma membrane requires the exocyst complex (Langevin et al., 2005) and that this complex is physically associated to Rab11 (Beronja et al., 2005). Furthermore, the exocyst is linked to the actin cytoskeleton (Heider and Munson, 2012) and several lines of evidence point to a role of FGF signaling in modulation of actin cytoskeleton dynamics (Muha and Muller, 2013). Hence, blocking FGF signaling could reduce cytoskeleton dynamics and indirectly block or diminish Rab11–exocyst trafficking of E-cadherin. This mechanism could also have a contribution from Rac signaling, given that all these regulators are in place for regulation of endosome levels in border cells (Wan et al., 2013). It would be of great interest to explore the molecular mechanism by which FGF modulates trafficking of zygotic E-cadherin.

We show that FGF-dependent pmg pocket formation has repercussions for PGC clustering and movement across the midgut epithelium. The FGF-dependent defects are present specifically at the blind end of the pmg, which is also the domain of active FGF signaling, as seen through dpERK activation. We show that FGF signaling modulates localization of new E-cadherin to the adhesive belt. As a result, in FGF mutants, pmg tissue loses integrity and the pmg pocket collapses, pushing PGCs to ectopic anterior regions. We propose that, as a result of pmg collapse, two outputs lead, indirectly, to PGC impaired movement (Figs 6 and 7). First, PGCs disperse and adhere to more anterior regions of the midgut that are outside the FGF domain of action and have higher levels of E-cadherin, too far from the region of ICP delamination to move through. Second, tissue folds created by pmg collapse trap PGCs in a midgut region outside the FGF domain that still retains its epithelial character and is now forming ectopic adhesions. It is unclear why FGF signaling is activated in such a specific domain of the pmg and what could be its functional significance. Interestingly, although in *shg* zygotic mutants, presumably, E-cadherin is reduced in all cells, these embryos also show stronger pmg defects in the ventral region. A possible scenario is that this region requires stronger cell bonds to maintain tissue 3D shape during pmg morphogenesis, requiring additional adhesion regulation.

The formation of the pmg pocket concomitant with the clustering of PGCs within its lumen likely ensures the organized transport of these cells inside the embryo. Specifically the concavity of the lumen seems to be important for ensuring the delivery of PGC to its blind end, where the cluster can reside and where remodeling of the pmg and simultaneous migration of PGCs takes place.

We uncovered a new function of FGF signaling for maintenance of cell adhesion. We show that upon loss of Btl–Bnl signaling in its domain in the pmg the tissue loses its columnar shape and cells adopt cuboidal and round shapes, suggestive of loss of cell adhesion (Fig. S4). The 3D and dynamic nature of the pmg tissue does not allow a consistent, detailed analysis of cell adhesions at the cellular level. To test whether loss of FGF signaling is sufficient to induce loss of cell adhesion and, importantly, to test whether FGF signaling has a global role on maintenance of cell adhesion, we analyzed the embryonic ventral ectoderm, a tissue that also requires both maternal and zygotic E-cadherin (Tepass et al., 1996) and expresses Btl endogenously (Shishido et al., 1993). We show that this tissue also requires Btl signaling to maintain cell adhesion (Fig. 8). It is possible that other morphogenetically active epithelial tissues with higher adhesive needs would also require FGF signaling for maintenance of cell adhesion.

Interestingly, in the pmg and ventral ectoderm during development, FGF signaling is needed to maintain cell adhesion, whereas during EMT in cancer cells, where FGFs are upregulated (Thiery et al., 2009; Wesche et al., 2011), FGFs maintain cells in a non-epithelial state. Although a role for FGF signaling in loss of cell adhesion is well established, there is some evidence emerging for a role of FGFs in cell adhesion in both vertebrate and invertebrate systems (Bae et al., 2012; Murakami et al., 2008). It remains to be explored what defines each biological output, but overall we conclude that FGF might be an important modulator of E-cadherin mediated cell adhesion across systems.

MATERIALS AND METHODS

Drosophila genetics

All experiments were carried out at 25°C, unless stated. The following stocks were used: yw^{1118} was used as WT strain, *btl-GAL4,UASp-Act5C-GFP*, *P(5′ lwB)*$btl^{H82\Delta3}$ (*btl* hypomorphic allele; Klambt et al., 1992), bnl^{P1} (bnl^{00857}, null allele; Sutherland et al., 1996), bnl^{P2} (bnl^{06916}, hypomorphic allele; Sutherland et al., 1996), *w; UAS-btl*$^{\lambda}$, *UAS-bnl*, *48Y-GAL4*, *UASCD8GFP* (Bloomington Stock Center), *UAStRab5*^{S43N} (DN), *UAStRab11*^{S25N} (DN), *UAStshi*^{DN} (provided by Enrique Martin-Blanco, IBMB, Barcelona, Spain), *P(lacZ) insc*^{AB44} (*inscuteable–lacZ*, provided by Ruth Lehmann, Department of Cell Biology, Kimmel Center for Biology and Medicine of the Skirball Institute, NY; Kraut and Campos-Ortega, 1996).

Two different alleles of trachealess were used: trh^{10512} and trh^{8} (provided by Marta Llimargas, IBMB, Barcelona, Spain; Isaac and Andrew, 1996; Wilk et al., 1996), *nullo-GAL4* (provided by Ruth Lehmann, originally from Walter Gehring, University of Basel, Switzerland and Eric Wieschaus, Princeton University, NJ, USA), *UAS-EcadGFP* (provided by Marta Llimargas; Oda and Tsukita, 1999), *DE-cad::GFP* (provided by Marta Llimargas; Huang et al., 2009), *en-GAL4, UASnlsGFP* (provided by A. Casali, IRB, Barcelona, Spain), $btl^{H82\Delta3}$, *UAS* btl^{DN}*/TM3* (provided by Jordi Casanova, IRB/IBMB, Barcelona, Spain), *torD4021/Ms(2)M,bwD/CyO* (male sterile source, provided by Jordi Casanova).

The E-cadherin-null and dominant-negative alleles, shg^{1H} and shg^{G317}, were provided by Marta Llimargas, originally characterized by the Hartenstein laboratory using alleles from Christiane Nüsslein-Volhard (Tepass et al., 1996). The following stocks were made with standard genetics techniques: *48Y-GAL4;* bnl^{P1}*; w; nullo-GAL4, UAS-EcadGFP; nos-GAL4, UAS-RedStinger*.

RNA sample collections

For collection of unfertilized eggs, *yw* virgin females were crossed to *Ms(2)M,bw/CyO* sterile males and 2 h collections of eggs were made 2–3 days after the initial crossing. For the 2–3 h collection of fertilized embryos, *yw* females (with *yw* males) were allowed to lay eggs for 1 h and these were aged in the plate for an additional 2 h.

In all cases, the first two to three plates of eggs or embryos were discarded to avoid collection of retained eggs. Three independent collections for RNA extractions were made for either fertilized or unfertilized eggs. Total RNA was extracted using TRIzol (Invitrogen) with a double precipitation protocol and PelletPaint Coprecipitant (Novagen). RNA was quantified with a nanodrop spectrophotometer (ThermoScientific) and treated with RNase-free DNase (Roche) to eliminate possible genomic DNA contamination.

RT-PCR and qRT-PCR

For PCR amplifications, 60 ng to 4 µg of RNA was used to synthesize complementary DNA (cDNA) using Revertaid H minus First Strand cDNA kit with oligo d(T) (Thermo Scientific). For each experimental condition, a minimum of three technical replicates were performed on three biological replicate samples. For *bnl*, nine technical replicates (three independent PCR reactions) were performed, and for *kr* and *rp49* six technical replicates (two independent PCR reactions) were performed. qRT-PCR reactions were carried out using LightCycler480 and SYBR green I master (Roche). The *bnl*

Journal of Cell Science

transcript fold change between fertilized and unfertilized samples was determined using the ΔΔCt method with the stable *rp49* transcript as reference.

Regular PCR was carried out using TAQ polymerase (Biotools) and product was run in 1% agarose gel with GelRed (Biotium). Primer sequences are listed in Table S1. $bnl^{(1)}$ primers were used for both regular and qPCR and $bnl^{(2)}$ primers were used for regular PCR, as additional confirmation of presence of *bnl* transcripts in unfertilized embryos.

Whole-mount immunostainings

Immunostainings were carried out using standard methods. The primary antibodies used were: mouse anti-1G9 (1:20, DSHB), rabbit anti-Vasa (1:2500, a gift of Anne Williamson and Helene Zinszner, NYU Medical Center, New York, NY), rat anti-DE-cad2 (1:20, DSHB), goat anti-GFP (1:600, Abcam), mouse anti-β-Gal (1:1000, Promega), rabbit anti-dpERK (1:50, Cell Signaling), mouse anti-Armadillo (1:20, DSHB), mouse anti-Neurotactin (1:10, DSHB), mouse anti-Fasciclin III (1:10, DSHB) and mouse anti-clift (eya) (1:50, DSHB) antibodies.

E-cadherin immunostainings were optimized to allow detection of protein in midgut tissues: embryos were freshly fixed for 10 min and left in primary antibody for 2 to 3 days.

TUNEL was performed using the In Situ Cell Death Detection kit (Roche), following the manufacturer's manual.

Embryo mounting, microscopy and image acquisition

Mounting of embryos for 3D reconstructions was adjusted to prevent flattening of 3D structures. Embryos were aligned dorsally or laterally, Immersol 518F oil was loaded on top and the embryos were then imaged directly using a 63× oil objective. Embryo imaging and acquisition was performed in a Leica TCS SPE Confocal microscope and image processing was carried out using ImageJ 1.45 S (NIH, USA) and Imaris 7.6 (Bitplane) software.

Quantification of pmg defects

For quantification of pmg defects at stage 9, in *bnl* and *btl* mutant embryos or embryos expressing $Rab11^{DN}$, $Rab5^{DN}$ and shi^{DN} in the midgut, embryos were stained for E-cadherin and all extent of the pmg tissue was analyzed for adhesive cable breakage and absence of E-cadherin spots at adherens junctions. A phenotype (defective adhesive cable) was considered when there was cable breakage on ventral region (area of Btl–Bnl activity), as shown in Figs 3 and 4, in which both these defects were simultaneously present: (1) loss of E-cadherin spots at the apical cable, being either distributed uniformly around the cell or absent (along the whole ventral area) and (2) loss of columnar epithelial cell shape (with a concomitant change to cuboidal).

Statistical significance of phenotype in mutant embryos as compared to control was evaluated using a χ^2 test.

Statistical analyses

We analyzed three or more independent experiments (except for shi^{DN} in Fig. 4E, in which two experiments were performed), and used Student's *t*-tests with a one-tailed distribution to assess the significance of PGC migration phenotypes and a χ^2 test to assess significance for the presence or absence of phenotype. Significance was considered when $P<0.001$ (***) or $P<0.01$ (**).

Acknowledgements

We thank M. Llimargas, J. Seifert, S. Marques and P. Okenve for critical reading of the manuscript and J. Casanova and P. Rangan for discussions. We thank N. Luque and E. Fuentes for technical assistance. We thank Developmental Studies Hybridoma Bank for antibodies and the Bloomington stock collection, R. Lehmann, M. Llimargas and J. Casanova for flies.

Competing interests

The authors declare no competing or financial interests.

Author contributions

S.R. conceived the project. S.R. and G.P. carried out the experiments. S.R. analyzed the data, with the help of G.P. S.R. wrote the paper.

Funding

This work was supported by funds of Ministerio de Ciencia e Innovacion [grant number BFU2012-39509-C02-02 to S.R.]; and the European Union Research Executive Agency [grant number PEOPLE-CIG/1816 to S.R.].

Supplementary information

Supplementary information available online at
http://jcs.biologists.org/lookup/suppl/doi:10.1242/jcs.174284/-/DC1

References

Adams, C. L. and Nelson, W. J. (1998). Cytomechanics of cadherin-mediated cell-cell adhesion. *Curr. Opin. Cell Biol.* **10**, 572-577.

Bae, Y.-K., Trisnadi, N., Kadam, S. and Stathopoulos, A. (2012). The role of FGF signaling in guiding coordinate movement of cell groups: guidance cue and cell adhesion regulator? *Cell Adh. Migr.* **6**, 397-403.

Beronja, S., Laprise, P., Papoulas, O., Pellikka, M., Sisson, J. and Tepass, U. (2005). Essential function of Drosophila Sec6 in apical exocytosis of epithelial photoreceptor cells. *J. Cell Biol.* **169**, 635-646.

Chihara, T., Kato, K., Taniguchi, M., Ng, J. and Hayashi, S. (2003). Rac promotes epithelial cell rearrangement during tracheal tubulogenesis in Drosophila. *Development* **130**, 1419-1428.

Costa, M., Wilson, E. T. and Wieschaus, E. (1994). A putative cell signal encoded by the folded gastrulation gene coordinates cell shape changes during Drosophila gastrulation. *Cell* **76**, 1075-1089.

De Renzis, S., Elemento, O., Tavazoie, S. and Wieschaus, E. F. (2007). Unmasking activation of the zygotic genome using chromosomal deletions in the Drosophila embryo. *PLoS Biol.* **5**, e117.

DeGennaro, M., Hurd, T. R., Siekhaus, D. E., Biteau, B., Jasper, H. and Lehmann, R. (2011). Peroxiredoxin stabilization of E-cadherin promotes primordial germ cell adhesion. *Dev. Cell* **20**, 233-243.

Desclozeaux, M., Venturato, J., Wylie, F. G., Kay, J. G., Joseph, S. R., Le, H. T. and Stow, J. L. (2008). Active Rab11 and functional recycling endosome are required for E-cadherin trafficking and lumen formation during epithelial morphogenesis. *Am. J. Physiol. Cell Physiol.* **295**, C545-C556.

Gabay, L., Seger, R. and Shilo, B. Z. (1997). MAP kinase in situ activation atlas during Drosophila embryogenesis. *Development* **124**, 3535-3541.

Heider, M. R. and Munson, M. (2012). Exorcising the exocyst complex. *Traffic* **13**, 898-907.

Huang, J., Zhou, W., Dong, W., Watson, A. M. and Hong, Y. (2009). Directed, efficient, and versatile modifications of the Drosophila genome by genomic engineering. *Proc. Natl. Acad. Sci. USA* **106**, 8284-8289.

Isaac, D. D. and Andrew, D. J. (1996). Tubulogenesis in Drosophila: a requirement for the trachealess gene product. *Genes Dev.* **10**, 103-117.

Kamei, T., Matozaki, T., Sakisaka, T., Kodama, A., Yokoyama, S., Peng, Y.-F., Nakano, K., Takaishi, K. and Takai, Y. (1999). Coendocytosis of cadherin and c-Met coupled to disruption of cell-cell adhesion in MDCK cells–regulation by Rho, Rac and Rab small G proteins. *Oncogene* **18**, 6776-6784.

Klambt, C., Glazer, L. and Shilo, B. Z. (1992). breathless, a Drosophila FGF receptor homolog, is essential for migration of tracheal and specific midline glial cells. *Genes Dev.* **6**, 1668-1678.

Kraut, R. and Campos-Ortega, J. A. (1996). inscuteable, a neural precursor gene of Drosophila, encodes a candidate for a cytoskeleton adaptor protein. *Dev. Biol.* **174**, 65-81.

Kunwar, P. S., Sano, H., Renault, A. D., Barbosa, V., Fuse, N. and Lehmann, R. (2008). Tre1 GPCR initiates germ cell transepithelial migration by regulating Drosophila melanogaster E-cadherin. *J. Cell Biol.* **183**, 157-168.

Langevin, J., Morgan, M. J., Rossé, C., Racine, V., Sibarita, J.-B., Aresta, S., Murthy, M., Schwarz, T., Camonis, J. and Bellaïche, Y. (2005). Drosophila exocyst components Sec5, Sec6, and Sec15 regulate E-cadherin trafficking from recycling endosomes to the plasma membrane. *Dev. Cell* **9**, 365-376.

Le, T. L., Yap, A. S. and Stow, J. L. (1999). Recycling of E-cadherin: a potential mechanism for regulating cadherin dynamics. *J. Cell Biol.* **146**, 219-232.

Lecuit, T. and Lenne, P.-F. (2007). Cell surface mechanics and the control of cell shape, tissue patterns and morphogenesis. *Nat. Rev. Mol. Cell Biol.* **8**, 633-644.

Lock, J. G. and Stow, J. L. (2005). Rab11 in recycling endosomes regulates the sorting and basolateral transport of E-cadherin. *Mol. Biol. Cell* **16**, 1744-1755.

Maitre, J.-L. and Heisenberg, C.-P. (2013). Three functions of cadherins in cell adhesion. *Curr. Biol.* **23**, R626-R633.

Muha, V. and Muller, H.-A. (2013). Functions and mechanisms of Fibroblast Growth Factor (FGF) signalling in Drosophila melanogaster. *Int. J. Mol. Sci.* **14**, 5920-5937.

Murakami, M., Nguyen, L. T., Zhuang, Z. W., Moodie, K. L., Carmeliet, P., Stan, R. V. and Simons, M. (2008). The FGF system has a key role in regulating vascular integrity. *J. Clin. Invest.* **118**, 3355-3366.

Oda, H. and Tsukita, S. (1999). Nonchordate classic cadherins have a structurally and functionally unique domain that is absent from chordate classic cadherins. *Dev. Biol.* **216**, 406-422.

Palacios, F., Tushir, J. S., Fujita, Y. and D'Souza-Schorey, C. (2005). Lysosomal targeting of E-cadherin: a unique mechanism for the down-regulation of cell-cell

adhesion during epithelial to mesenchymal transitions. *Mol. Cell. Biol.* **25**, 389-402.
Pilot, F. and Lecuit, T. (2005). Compartmentalized morphogenesis in epithelia: from cell to tissue shape. *Dev. Dyn.* **232**, 685-694.
Satoh, A. K., O'Tousa, J. E., Ozaki, K. and Ready, D. F. (2005). Rab11 mediates post-Golgi trafficking of rhodopsin to the photosensitive apical membrane of Drosophila photoreceptors. *Development* **132**, 1487-1497.
Seifert, J. R. K. and Lehmann, R. (2012). Drosophila primordial germ cell migration requires epithelial remodeling of the endoderm. *Development* **139**, 2101-2106.
Semotok, J. L., Westwood, J. T., Goldman, A. L., Cooperstock, R. L. and Lipshitz, H. D. (2008). Measuring mRNA stability during early Drosophila embryogenesis. *Methods Enzymol.* **448**, 299-334.
Shilo, B. Z. (2014). The regulation and functions of MAPK pathways in Drosophila. *Methods* **68**, 151-159.
Shimizu, H., Kawamura, S. and Ozaki, K. (2003). An essential role of Rab5 in uniformity of synaptic vesicle size. *J. Cell Sci.* **116**, 3583-3590.
Shishido, E., Higashijima, S., Emori, Y. and Saigo, K. (1993). Two FGF-receptor homologues of Drosophila: one is expressed in mesodermal primordium in early embryos. *Development* **117**, 751-761.
Sutherland, D., Samakovlis, C. and Krasnow, M. A. (1996). branchless encodes a Drosophila FGF homolog that controls tracheal cell migration and the pattern of branching. *Cell* **87**, 1091-1101.
Sweeton, D., Parks, S., Costa, M. and Wieschaus, E. (1991). Gastrulation in Drosophila: the formation of the ventral furrow and posterior midgut invaginations. *Development* **112**, 775-789.
Tepass, U. (1996). Crumbs, a component of the apical membrane, is required for zonula adherens formation in primary epithelia of Drosophila. *Dev. Biol.* **177**, 217-225.
Tepass, U. and Hartenstein, V. (1994). The development of cellular junctions in the Drosophila embryo. *Dev. Biol.* **161**, 563-596.
Tepass, U. and Hartenstein, V. (1995). Neurogenic and proneural genes control cell fate specification in the Drosophila endoderm. *Development* **121**, 393-405.
Tepass, U., Gruszynski-DeFeo, E., Haag, T. A., Omatyar, L., Torok, T. and Hartenstein, V. (1996). shotgun encodes Drosophila E-cadherin and is preferentially required during cell rearrangement in the neurectoderm and other morphogenetically active epithelia. *Genes Dev.* **10**, 672-685.
Thiery, J. P., Acloque, H., Huang, R. Y. J. and Nieto, M. A. (2009). Epithelial-mesenchymal transitions in development and disease. *Cell* **139**, 871-890.
Thomsen, S., Anders, S., Janga, S. C., Huber, W. and Alonso, C. R. (2010). Genome-wide analysis of mRNA decay patterns during early Drosophila development. *Genome Biol.* **11**, R93.
Uemura, T., Oda, H., Kraut, R., Hayashi, S., Kotaoka, Y. and Takeichi, M. (1996). Zygotic Drosophila E-cadherin expression is required for processes of dynamic epithelial cell rearrangement in the Drosophila embryo. *Genes Dev.* **10**, 659-671.
Wan, P., Wang, D., Luo, J., Chu, D., Wang, H., Zhang, L. and Chen, J. (2013). Guidance receptor promotes the asymmetric distribution of exocyst and recycling endosome during collective cell migration. *Development* **140**, 4797-4806.
Wesche, J., Haglund, K. and Haugsten, E. M. (2011). Fibroblast growth factors and their receptors in cancer. *Biochem. J.* **437**, 199-213.
Wilk, R., Weizman, I. and Shilo, B. Z. (1996). trachealess encodes a bHLH-PAS protein that is an inducer of tracheal cell fates in Drosophila. *Genes Dev.* **10**, 93-102.
Wirtz-Peitz, F. and Zallen, J. A. (2009). Junctional trafficking and epithelial morphogenesis. *Curr. Opin. Genet. Dev.* **19**, 350-356.
Zerial, M. and McBride, H. (2001). Rab proteins as membrane organizers. *Nat. Rev. Mol. Cell Biol.* **2**, 107-117.

Journal of Cell Science